Toll-like receptor 5-mediated signaling enhances liver regeneration in mice

Wen Zhang
Tianjin University
Lei Wang
National Center of Protein Sciences Beijing
Xue-Hua Sun
Tianjin University
Xian Liu
National Center of Protein Sciences Beijing
Yang Xiao
National Center of Protein Sciences Beijing
Jie Zhang
Tianjin University
Ting Wang
Anhui Medical University
Hui Chen
National Center of Protein Sciences Beijing
Yi-Qun Zhan
National Center of Protein Sciences Beijing
Miao Yu
National Center of Protein Sciences Beijing
Chang-Hui Ge
Beijing Institute of Radiation Medicine
Chang-Yan Li
National Center of Protein Sciences Beijing
Guang-Ming Ren
National Center of Protein Sciences Beijing
Rong-Hua Yin
National Center of Protein Sciences Beijing
Xiao-Ming Yang (xiaomingyang@sina.com)
National Center of Protein Sciences Beijing https://orcid.org/0000-0003-3629-0946

Research

Keywords: Toll-like receptor 5, CBLB502, NF-κB, partial hepatectomy, liver regeneration

Posted Date: August 5th, 2020

DOI: https://doi.org/10.21203/rs.3.rs-53389/v1

Version of Record: A version of this preprint was published on February 23rd, 2021. See the published version at https://doi.org/10.1186/s40779-021-00309-4.

Abstract

Background

Toll-like receptor 5 (TLR5)-mediated pathways play critical roles in regulating hepatic immune response and show hepatoprotective effect in mouse models of liver injury. However, the role of TLR5 in experimental models of liver regeneration has not been investigated. This study aims to determine the role of TLR5 in the partial hepatectomy (PHx)-induced liver regeneration.

Methods

We performed 2/3 PHx in wild-type (WT) mice, TLR5 knockout mice, or TLR5 agonist CBLB502 treated mice as an established model of liver regeneration. Bacterial flagellin content was measured by ELISA, and hepatic TLR5 expression was determined by real-time PCR analyses and flow cytometry. To study the effects of TLR5 on hepatocyte proliferation, proliferating cell nuclear antigen (PCNA) and the incorporation of bromodeoxyuridine (BrdU) were analyzed by immunohistochemistry (IHC) staining. The role of TLR5 in the priming of liver regeneration was examined by real-time PCR analyses of immediate early gene mRNA levels, as well as western blot analysis of hepatic NF-κB and STAT3 activation. Cytokines and growth factors production after PHx were detected using real-time PCR analyses and cytometric bead array (CBA) assays. Oil Red O staining and hepatic lipids concentrations were analyzed to examine the effect of TLR5 on hepatic lipid accumulation after PHx.

Results

The bacterial flagellin content in serum and liver was increased and the hepatic TLR5 expression was significantly up-regulated in WT mice upon PHx. TLR5-deficient mice exhibited reduced numbers of BrdU- and PCNA-positive cells, suppressed immediate early gene expression, and decreased cytokines and growth factors production. Moreover, PHx-induced NF-κB and STAT3 activation was inhibited in the liver of *Tlr5*$^{-/-}$ mice compared with WT mice. Consistently, administration of CBLB502 significantly promoted PHx-mediated hepatocyte proliferation correlated with enhanced production of proinflammatory cytokines and recruitment of macrophages and neutrophils in liver. In addition, *Tlr5*$^{-/-}$ mice displayed significantly decreased hepatic lipids concentrations and Oil Red O positive areas compared with WT mice after PHx.

Conclusions

We reveal that TLR5 activation is involved in the initial events of liver regeneration after PHx. Our results demonstrate that TLR5 signaling positively regulates liver regeneration and suggest a potential application of TLR5 agonist in promoting liver regeneration.

Background

The liver is a unique organ that has a great ability to regenerate by itself when a massive loss of hepatic parenchymal cells happens upon hepatic resection [1]. Liver regeneration following partial hepatectomy (PHx) occurs in a multi-step process with at least three important recovery phases: the priming phase, the proliferation phase, and the termination phase [2]. The initiation of liver regeneration is termed the priming phase, in which proinflammatory cytokines such as tumor necrosis factor-α (TNF-α) and interleukin-6 (IL-6) are secreted from nonparenchymal cells such as Kupffer cells (KCs) and sinusoidal epithelial cells to stimulate normally quiescent hepatocytes and enable these cells to gain proliferative competence and become responsive to hepatic growth factors [3–5]. One hallmark of the priming phase is the induction of proinflammatory cytokines and immediate early genes such as the proto-oncogenes c-*myc, c-fos*, and c-*jun* [6]. However, the mechanisms by which PHx results in cytokine gene induction and transcription factor activation in the liver are still unclear.

Toll-like receptors (TLRs) act as innate immune signal sensors and play central roles in host defense, which are widely expressed on parenchymal and nonparenchymal liver cells [7, 8]. In addition to their roles in defense against pathogens, TLRs also significantly contribute to tissue repair and regeneration [9–11]. Myeloid differentiation factor 88 (MyD88) is a common adaptor molecule required for TLRs-mediated signaling pathways activation and proinflammatory cytokine production [12, 13]. MyD88 deletion impairs liver regeneration by attenuating NF-κB activation and decreasing immediately early gene expression and TNF-α and IL-6 production in KCs after PHx, which highlights that TLR/MyD88-mediated pathways are crucial for PHx-induced liver regeneration [14, 15]. However, further studies have excluded the possible contribution of TLR2, TLR4, or TLR9 to MyD88-mediated pathways in liver regeneration after PHx in mice [15]. In addition, TLR3 signaling which uses a distinct adaptor protein TRIF but not MyD88 was shown to attenuate the initiation of liver regeneration [16]. Therefore, liver regeneration is likely to be driven by some other TLRs via the MyD88 signaling pathway.

TLR5 serves as the main receptor for bacterial flagellin and plays a critical role in regulating the response to ionizing radiation [17, 18] and immune response [19–21]. CBLB502, a pharmacologically optimized flagellin derivative, has been reported to protect mice from lethal total-body irradiation-induced gastrointestinal and hematopoietic acute radiation syndromes [17] and ionizing radiation-induced male reproductive system damage [18]. In recent years, liver has been identified as one of the major organs responding to CBLB502. Administration of CBLB502 strongly activates NF-κB-, STAT3-, phenobarbital-responsive enhancer module (PREM)-, and activator protein 1 (AP-1)-driven pathways in liver, resulting in the induction of numerous immunomodulatory factors and massive recruitment of immune cells [22]. Moreover, TLR5-mediated pathways were shown to protect mice from anti-Fas antibody- or concanavalin A (Con A)-induced fulminant liver injury by limiting hepatocytes apoptosis or T/NKT cell activity [22, 23]. In addition, our own and others' studies have indicated that TLR5 signaling serves as a regulator in hepatic immune cell activation and cytokine production [22–25]. Importantly, injection of CBLB502 alone in wild-type (WT) mice induced rapid increase of serum or hepatic TNF-α, IL-6, and G-CSF, all of which are shown to contribute to liver regeneration [22, 26]. Together, these data suggest that TLR5-mediated

pathways may be involved in the regulation of liver regeneration. To the best of our knowledge, the effect of TLR5-medicated pathways on the experimental models of liver regeneration has not been studied previously. In this paper, we aimed to determine the role of TLR5 in the PHx-induced liver regeneration.

Methods

Animals

Tlr5$^{-/-}$ mice on a C57BL/6 background from Jackson Laboratory were kindly provided by Prof. Huimin Yan (Wuhan Institute of Virology, Chinese Academy of Sciences, Wuhan, China). Specific pathogen-free (SPF) C57BL/6 mice were purchased from Vital River Experimental Animal Company (Beijing, China). In all experiments, genetically modified mice were systematically compared to their age-, and weight-matched WT littermates. All animals were maintained in a temperature-controlled, specific pathogen-free room with a 12-hour light and dark cycle and *ad libitum* diet (standard laboratory chow and water) in the Experimental Animal Center of the Academy of Military Medical Sciences according to the National Laboratory Animal guidelines (Ministry of Health, P.R. China, 1998). All animal experiments were approved by the Institutional Animal Care and Use Committee of the Beijing Institute of Lifeomics.

Partial Hepatectomy Model

For 2/3 partial hepatectomy studies, male mice between 8 and 10 weeks of age were anesthetized and subjected to a midline laparotomy by aseptic extirpation of the median and left lateral lobes according to the procedure of Higgins and Anderson [27]. Control animals underwent midventral laparotomy without manipulation of the liver (sham surgery). Experiments began between 8:00 AM and 12:00 PM to minimize possible diurnal variations, and mice had access to food and water throughout the testing period. For CBLB502 administration, mice were pretreated with a single dose of CBLB502 (0.2 mg/kg) intraperitoneally 1 hour before partial hepatectomy.

Gene expression datasets

For gene expression analysis, a published dataset was downloaded from GEO repository (GSE95135). Raw data were normalized by the robust multiarray average (RMA) method. We use ExpressVis (http://www.fgvis.com/expressvis/) to visualize the expression of specific genes of interest [28].

Flow cytometry

Liver mononuclear cells (MNCs) were obtained as previously described [23]. Briefly, the liver tissue was dissected, and dissociated in 0.05% type IV collagenase (Sigma-Aldrich, C5138) digestion. Liver specimens were pressed through a 40 μm cell strainer. The single-cell suspension was centrifuged at 50 *g* for 5 min, and the supernatant was further centrifuged at 320 g for 5 minutes. The pellet containing liver mononuclear cells was resuspended in 10 ml of 30% Percoll (GE, 17089102), then centrifuged at 800 g for 15 minutes without brake. The cell pellet was washed with PBS and then treated with lysis solution

(TIANGEN Biotech, RT122) to remove red blood cells. Centrifuge at 400 *g* for 10 min, resuspend the mononuclear cell pellets in RPMI-1640 medium for Flow cytometric analysis. MNCs was stained with anti-mouse F4/80-FITC (eBioscience, 11-4801-82), anti-mouse CD45.2-PE-Cy7 (Biolegend,109830), anti-mouse Siglec F-APC (Biolegend, 155508), anti-mouse Ly6G-eFluor 450 (eBioscience, 48-9668-82), and anti-mouse CD11b-BV605 (Biolegend, 101257), anti-mouse TLR5-PE (Abcam, ab45119) or anti-mouse IgG2a (Abcam, ab91363). The number of MNCs was counted by 123-count eBeads Counting Beads (eBioscience, 01-1234). Flow cytometric analysis was performed using a BD FACSCalibur instrument (BD Bioscience) and FlowJo software (Tree Star, Ashland, OR).

Histological analysis, immunohistochemistry stainings, and Oil Red O staining

Liver tissues were excised and fixed in 4% paraformaldehyde and then embedded in paraffin. Sections were stained with hematoxylin and eosin (H&E) for morphological analysis. Liver tissues were frozen directly in OCT compound for Oil Red O staining. Liver regeneration rate was determined by the BrdU incorporation assay and proliferating cell nuclear antigen (PCNA) immunohistochemistry staining. For BrdU incorporation, 85 μg BrdU (Sigma, B5002) per gram body weight was injected intraperitoneally 2 hours before the mice were sacrificed, and incorporation was visualized immunohistochemically using BrdU immunohistochemistry staining. BrdU and PCNA immunohistochemistry staining were performed following standard protocols (Wuhan Servicebio technology co., LTD), and the percentage of positive cells were analyzed from randomly selected 3 fields of ×200 magnification for each sample. Oil Red O positive areas were quantified in 3 fields per slide under light microscopy (×200). All images of the liver sections were captured using Nikon Digital Sight DS-U3 camera. Image analysis procedures were performed with Image Pro Plus v6.0 (Media Cybernetics, Inc).

Measurements of Cytokines, flagellin concentrations, and aminotransferases

To detect the cytokines in serum, Cytometric bead array (CBA) Mouse TNF Flex Set (BD Biosciences, 558299), Mouse IL-6 Flex Set (BD Biosciences, 558301), Mouse G-CSF Flex Set (BD Biosciences, 560152), Mouse HGF ELISA kit (Abcam, ab223862), Mouse TGFa ELISA kit (Cloud-Clone Corp., SEA123Mu) were used according to manufacturer's instruction. We used mouse flagellin ELISA kit (Beijing chengzhikewei biotechnology Co., SU-BN28100) for the quantitative determination of serum and liver homogenates flagellin concentrations. Serum ALT and AST were measured according to the IFCC primary reference procedures at Beijing CIC Clinical Laboratory (Beijing, China).

Detection of lipids

Serum lipids quantification was performed with LabAssay™ Cholesterol kit (Wako, 294-65801), LabAssay™ Triglyceride kit (Wako, 290-63701), and LabAssay™ NEFA kit (Wako, 294-63601) following standard methods. Hepatic lipids were assayed using Triglyceride assay kit (Applygen Technologies, E1013), Cholesterol assay kit (Applygen Technologies, E1026), Free fatty acids assay kit (Applygen Technologies, E1000) according to the manufacturer's recommended protocol.

Real-time PCR

Total RNA was extracted by TRIzol (Thermo Fisher Scientific, 15596026) and reverse-transcribed using RevertAid First Strand cDNA Synthesis Kit (Thermo Fisher Scientific, K1622). The cDNAs were amplified with SYBR Green Realtime PCR Master Mix (TOYOBO, QPK-201) by LightCycler 480 real-time PCR detection system (Roche). Relative gene expression was evaluated by the ΔCT method, and *Actb* was used as an internal control. Genes specific primers were designed by Primer Bank and listed in Table S1 in Supplementary Information.

Western blot

Proteins were extracted from liver specimens homogenized with PBS containing 0.5% Triton X-100 and proteinase inhibitor cocktail (Roche, 04693116001). Liver total protein quantification was performed with the Pierce™ BCA Protein Assay Kit (Thermo Fisher Scientific, 23227). Protein extracts were denatured in Laemmli sample buffer and separated by SDS-PAGE. Proteins on the gel were transferred to a PVDF membrane and then probed with indicated primary antibodies. Immune complexes on the membrane were detected with HRP-conjugated secondary antibodies and enhanced chemiluminescence reagents (Thermo Fisher Scientific, 34580). The antibodies used were as follows: rabbit monoclonal anti-phospho-NF-κB p65 (Ser536) (Cell Signaling Technology, 3033), rabbit monoclonal anti-NF-κB p65 (Cell Signaling Technology, 8242), rabbit monoclonal anti-phospho-IκBα (Ser32) (Cell Signaling Technology, 2859), mouse monoclonal anti-IκBα (Cell Signaling Technology, 4814), mouse monoclonal anti-phospho-Stat3 (Tyr705) (Cell Signaling Technology, 9145), mouse monoclonal anti-Stat3 (Cell Signaling Technology, 9139), rabbit monoclonal anti-ACTB (ABclonal, AC026). Secondary HRP conjugated antibodies used were goat anti-mouse IgG (ABclonal, AS003), goat anti-rabbit IgG (ABclonal, AS014).

Statistics

Statistics were calculated with GraphPad Prism 7 (GraphPad Software). Results were expressed as means ± standard error of the mean (SEM). A standard two-tailed unpaired Student's *t*-test was used to test the significance of differences between two groups. The distribution of variables is tested by the Kolmogorov-Smirnov test. *P* value <0.05 was considered statistically significant.

Results

TLR5 is up-regulated in the liver after PHx

To determine the role of TLR5 in liver regeneration, we performed 2/3 PHx in C57BL/6 mice as an established model of liver regeneration [27]. Significant increases of bacterial flagellin in the serum and liver were observed at 6 hours post-PHx (Fig. 1a). We next investigated the expression pattern of TLR5 in the liver of mice after PHx. A global transcriptome analysis of the mouse liver at various time points following PHx revealed a significant up-regulation of TLR5 along with other TLRs (GSE95135) [29] (Fig. 1b). Consistently, real-time PCR analyses showed that the expression of TLR5 mRNA in the liver was

significantly increased following PHx, with two peaks occurring at 1 hour and 12 hours after PHx (Fig. 1c). By flow cytometry, we found that TLR5 was expressed in hepatic neutrophils, KCs and recruited macrophages (Fig. 1d-e), which is line with the previous results of our own and others [8, 23]. The mean fluorescence intensity of TLR5 in these cells was unchanged, but the number of neutrophils and recruited macrophages were significantly increased following PHx, which might account for the up-regulation of hepatic TLR5 expression in the early phase of liver regeneration (Fig. 1f).

TLR5 deficiency attenuates hepatocyte proliferation following PHx

To access the effect of TLR5 on liver regeneration, we performed 2/3 PHx in *Tlr5*$^{-/-}$ mice and their WT littermates. The hepatocyte proliferation, as assessed by the incorporation of bromodeoxyuridine (BrdU), was significantly decreased in *Tlr5*$^{-/-}$ mice compared to WT mice at 36 and 48 hours after PHx (Fig. 2a-b). Consistent with this result, proliferating cell nuclear antigen (PCNA) staining showed a statistically significant reduction in the number of proliferating hepatocytes in *Tlr5*$^{-/-}$ mice at 36 hours after PHx (Fig. 2c-d). The serum alanine transaminase (ALT) and aspartate transaminase (AST) levels were rapidly elevated in mice after PHx but were unaffected by TLR5 deficiency (Fig. 2e), indicating a similar degree of liver injury in the two genotypes. Together, these data suggest that deficiency of TLR5 significantly decreases hepatocyte proliferation in the first 48 hours after PHx.

TLR5 deficiencysuppresses hepatocyte priming in PHx-induced liver regeneration

As hepatic flagellin and TLR5 expression increased at early time points after PHx, we examined the effects of TLR5 on the priming of liver regeneration following PHx. Real-time PCR was used to determine the mRNA levels of genes involved in the initial stage of cell proliferation and the results showed that PHx increased the hepatic mRNA levels of c-Jun, c-Fos, and c-Myc in both *Tlr5*$^{-/-}$ and WT mice at 30 to 60 min following PHx, but the increase was significantly blunted in *Tlr5*$^{-/-}$ mice (Fig. 3a), suggesting loss of TLR5 suppresses PHx-induced immediate early gene expression.

We further investigated the effect of TLR5 signaling on proinflammatory cytokines expression upon PHx. As shown in Fig. 3b, serum levels of TNF-α, IL-6, TGF-α, and HGF in *Tlr5*$^{-/-}$ mice were similar to those in WT mice before PHx. PHx rapidly increased the serum levels of these cytokines in both WT and *Tlr5*$^{-/-}$ mice; however, these effects were greater in WT mice compared to those in *Tlr5*$^{-/-}$ mice at 6 and 12 hours after PHx (Fig. 3b). Consistently, the expression of TNF-α, IL-6, TGF-α, and HGF mRNA in liver was inhibited in *Tlr5*$^{-/-}$ mice at 1 and 3 hours after PHx (Fig. 3c). These results indicate that TLR5 signaling contributes to cytokines production induced by PHx.

Activation of NF-κB and STAT3 are well known as one of the major priming events during liver regeneration [6, 14]. NF-κB signaling pathway is activated in mouse liver by PHx as indicated by the phosphorylation and degradation of IκBα, and the phosphorylation of p65. Compared with WT mice, PHx-induced NF-κB activation in liver was inhibited in *Tlr5*$^{-/-}$ mice at 30 and 60 min after PHx (Fig. 3d). Both WT and *Tlr5*$^{-/-}$ mice displayed increased hepatic STAT3 phosphorylation levels at 30 and 60 min

following PHx, while *Tlr5*$^{-/-}$ mice showed lower levels of phosphorylated STAT3 than WT mice (Fig. 3d). Taken together, these findings indicate that TLR5 is involved in the regulation of hepatocyte priming in liver regeneration following PHx.

The TLR5 agonist CBLB502 enhances hepatocyte proliferation in mice following PHx

To further assess the role of TLR5 signaling in liver regeneration, we investigated whether administration of CBLB502, a TLR5 agonist derived from *Salmonella* flagellin, affects liver regeneration in mice after PHx. The liver/body weight ratio of CBLB502-pretreated mice was significantly higher than that of control mice during the first 72 hours post-PHx, suggesting that activation of TLR5 signaling pathway is involved in the early recovery of liver mass after PHx (Fig. 4a). Accordingly, PHx-induced liver damage was reduced by CBLB502 administration at 24 and 72 hours after PHx as revealed by decreased serum transaminases (Fig. 4b). Hepatocyte proliferation was markedly enhanced in CBLB502 treated mice at 36, 48, and 72 hours after hepatectomy by BrdU staining and at 36 and 48 hours by PCNA staining (Fig. 4c-f). Taken together, activation of TLR5 signaling by CBLB502 enhances hepatocyte proliferation in mice following PHx.

Enhanced inflammatory response in CBLB502-pretreated mice after PHx

In line with previous reports [23], injection of CBLB502 alone in WT mice induced rapid increases of serum TNF-α, IL-6, and G-CSF (Fig. 5a). Interestingly, TGF-α and HGF, which are critical for liver regeneration [30, 31], were also significantly up-regulated in the serum at 3 and 6 hours after CBLB502 injection (Fig. 5b). We next performed PHx 1 hour after CBLB502 administration. Much higher levels of serum TNF-α, IL-6, G-CSF, TGF-α, and HGF were observed in CBLB502-pretreated mice than in control mice right before PHx (Fig. 5c-d). After PHx, the serum levels of these growth factors were significantly increased in control mice, but the concentrations were still much lower than those in CBLB502-pretreated mice at 6 hours after PHx (Fig. 5c-d). Moreover, administration of CBLB502 significantly increased hepatic expression of c-Fos, c-Myc, c-Jun, TNF-α, and IL-6 mRNA at 1 hour post-PHx (Fig. 5e), which is consistent with the results in *Tlr5*$^{-/-}$ mice. We next examined whether CBLB502 affects the hepatic recruitment of immune cells after PHx. As shown in Fig. 5f, the number of mononuclear cells (MNCs), neutrophils and recruited macrophages in the liver was much higher in CBLB502 treated mice than in control mice before PHx, which was in line with previous reports that CBLB502 treatment induces recruitment of various types of immune cells into liver [22, 23]. PHx also induced a significant increase in the total number of hepatic MNCs, as well as the number of recruited macrophages and neutrophils in the liver, and mice pretreated with CBLB502 showed further increased number of these cells compared to mice pretreated with PBS. However, the number of KCs was not affected (Fig. 5f). Taken together, these data indicate that CBLB502 pretreatment increases hepatic inflammatory response in mice after PHx.

TLR5 signaling contributes to hepatic lipid accumulation induced by PHx

Liver transiently accumulates lipids during liver regeneration, which is associated with hepatocyte proliferation [32-34]. Histological analysis and Oil Red O staining showed an obvious decrease of hepatic

lipid accumulation in *Tlr5*$^{-/-}$ mice at 24 hours after PHx (Fig. 6a). The levels of triglyceride, free fatty acids, and cholesterol in liver homogenates were comparable between WT and *Tlr5*$^{-/-}$ mice under normal condition (Fig. 6b). Significant increases of triglyceride and free fatty acids levels in liver homogenates were observed in both WT and *Tlr5*$^{-/-}$ mice at 24 hours after PHx, but these increases were suppressed in *Tlr5*$^{-/-}$ mice (Fig. 6b). Deficiency of TLR5 did not affect the levels of hepatic cholesterol and serum triglyceride, free fatty acids, and cholesterol no matter before or after PHx (Fig. 6b-c). Consistent with these results, CBLB502 treatment increased hepatic triglyceride and free fatty acids accumulation at 24 and 36 hours following PHx, but had no significant effect on hepatic cholesterol content (Fig. 6d). Histological examination and Oil Red O staining of liver sections from CBLB502-treated and WT mice at different time points after PHx further confirmed these results (Fig. 6e). Collectively, these data suggest that TLR5 signaling pathway is required for the transient accumulation of fat in the liver after PHx.

Discussion

Although previous studies have shown that activation of TLR5 signaling has a significant effect on immune-privileged status of the liver and protects against ConA and Fas-agonistic antibodies-induced liver injury [19–23], the role of TLR5 signaling in liver regeneration has not been reported. In this study, we have identified a role for TLR5 in liver regeneration using TLR5 knockout mice and TLR5 agonist CBLB502 treated mice. We provided several lines of evidence suggesting that the activation of TLR5 signaling positively regulates liver regeneration via enhancing NF-κB and STAT3 activity and proinflammatory response in liver. First, bacterial flagellin content was increased in serum and liver after PHx. Meanwhile, the expression of TLR5 in the liver was significantly up-regulated. Second, loss of TLR5 resulted in inhibition of PHx-induced liver regeneration, which is associated with attenuation of NF-κB and STAT3 activation, proinflammatory cytokines production, and immediate early gene expression. Third, activation of TLR5 signaling by TLR5 agonist CBLB502 significantly promoted PHx-mediated hepatocytes proliferation, which is accompanied by enhanced production of proinflammatory cytokines and recruitment of macrophages and neutrophils in liver. Microbiota composition alteration is associated with higher levels of fecal bioactive lipopolysaccharide (LPS) and flagellin, which may affect liver regeneration. In the present study, we treated mice with gentamycin as previously described, which results in comparable microbial composition in the intestinal tract between WT mice and *Tlr5*$^{-/-}$ mice [23], thereby eliminates the effect of intestinal pathogenic bacteria on PHx-induced liver regeneration in *Tlr5*$^{-/-}$ mice. To our knowledge, this study is the first report that TLR5 is required for liver regeneration after PHx. CBLB502 is a rationally designed derivative of *Salmonella* flagellin that is substantially less immunogenic than full-length flagellin but retains its TLR5-dependent NF-κB-inducing activity, and it is currently under development as a medical radiation countermeasure and antitumor drug [17, 22, 24]. Our own studies have shown that CBLB502-mediated protective effects against Con A-induced hepatitis and ionizing radiation-induced male reproductive system damage were primarily dependent on the TLR5 signaling pathway [18, 23], which was in line with previous report that radioprotection by CBLB502 is indeed TLR5-dependent [17]. Thus, our findings that CBLB502 significantly promotes liver regeneration, together with that CBLB502 was shown to be effective as a tissue protectant in mouse models of liver

injury [23, 35, 36], suggest that activation of TLR5 signaling may have the potential for the improvement of liver regeneration when the liver is compromised.

It is well known that several cytokines such as TNF-α and IL-6 produced by nonparenchymal liver cells and transcription factors such as NF-κB and STAT3 are crucial for liver regeneration. After PHx, TLR/MyD88-mediated pathways activate NF-κB pathways in nonparenchymal liver cells, induce IL-6 and TNF-α production, and trigger immediate early gene expression in hepatocytes [3, 6, 14]. In TLR5 knockout mice, initiation of liver regeneration is abated at the earlier time point as evidence by suppression of NF-κB and STAT3 activation, TNF-α and IL-6 production, and immediate early gene expression after PHx, suggesting that TLR5 signaling is required for liver regeneration, especially for the priming phase. This conclusion is supported by the fact that CBLB502 treatment enhanced hepatic c-Myc, c-Fos, c-Jun, TNF-α, and IL-6 expression in mice in the early post-PHx period. Although Burdelya *et al* reported that hepatocytes were the main cell type directly and specifically responding to systemic administration of CBLB502 [22], previous studies showed a very low level of TLR5 expression in hepatocytes, as well as a fairly weak response of hepatocytes to CBLB502 *in vivo* [23, 37], which indicate TLR5 signaling may regulate PHx-induced liver regeneration through nonparenchymal liver cells. It is now almost universally accepted that the activation of NF-κB in KCs is crucial for intact liver regeneration after PHx [3, 6, 38]. Importantly, KCs were shown to express TLR5 in our present study, which is consistent with previous works [8]. Although the number of KCs in the liver and the expression of TLR5 in KCs were unaltered after PHx, the level of bacterial flagellin in serum and liver was increased in PHx-treated mice. Thus, the activation of TLR5 signaling in KCs may be enhanced following PHx and contribute to liver regeneration. In addition, hepatic recruited macrophages and neutrophils, which were shown to express TLR5 [8, 23], have been demonstrated to accelerate liver regeneration via the TNF/FasL/Fas or STAT3 pathway[39, 40]. After PHx, the expression level of TLR5 in recruited macrophages and neutrophils was not altered, but their number was significantly increased, suggesting that the up-regulation of hepatic TLR5 expression induced by PHx may be attributed to the influx of TLR5-positive immune cells. Studies of our own and others showed that administration of CBLB502 rapidly induced the expression of numerous immunomodulatory factors including TNF-α and IL-6 and massive recruitment of various types of immune cells such as macrophages and neutrophils in the liver of mice without PHx [22, 23], and the extent was further enhanced in the case of PHx. Therefore, it is possible that the early, transient, and controlled activation in hepatic TLR5 after PHx increases inflammation response during liver regeneration, by which TLR5 signaling promotes liver regeneration.

Except for TNF-α and IL-6, TLR5 signaling also affected TGF-α, HGF, and G-CSF expression after PHx. A marked decrease in systemic and liver local TGF-α, HGF, and G-CSF was detected in TLR5 knockout mice after PHx. In contrast, CBLB502 pretreatment significantly increased their expression. TGF-α is an autocrine stimulator of hepatocyte proliferation [31, 41]; HGF is produced in the liver by nonparenchymal cells and acts as a complete mitogen to promote hepatocytes proliferation through a paracrine mechanism [30, 42]. Their important roles in liver regeneration have been extensively reported [1–3, 41, 42]. These findings indicate that TLR5 signaling also regulates the proliferation phase of liver regeneration through induction of hepatocyte proliferation-associated growth factors. Induction of G-CSF

by CBLB502 plays an important role in the drug's ability to protect mice against radiation injury [17]. Previous studies also showed that G-CSF facilitates liver regeneration by suppression of hepatic NK cells and increasing the migration of BM-derived progenitors to the liver [43, 44]. Our previous studies showed that TLR5 signaling can restrain T/NKT cell activation in liver [23]. These data indicate that TLR5 signaling-induced facilitation of liver regeneration may also be achieved by immunoregulation of NK or/and NKT cells. Transient hepatic lipid accumulation during liver regeneration is essential for hepatocyte proliferation induced by PHx [32–34, 45]. Our results showed that TLR5 signaling significantly increases the levels of TG and free fatty acids in early regenerating liver, indicating that TLR5 signaling may contribute to lipid accumulation during early liver regeneration. Future studies could focus on deepening these findings.

Conclusion

The present work provides certain evidences that TLR5 activation is involved in the initial events of liver regeneration after PHx. Our findings open a new door for a better comprehension of the mechanisms of liver regeneration and suggest a potential application of TLR5 agonist in promoting liver regeneration.

Abbreviations

ALT: Alanine transaminase; AST:Aspartate transaminase; BrdU:Bromodeoxyuridine; CBA:Cytometric bead array; Con A:Concanavalin A; H&E:Hematoxylin and eosin; IHC:Immunohistochemistry; IL-6:Interleukin-6; KCs:Kupffer cells; MNCs:Mononuclear cells; MyD88:Myeloid differentiation factor 88; PCNA:Proliferating cell nuclear antigen; PHx:Partial hepatectomy; SEM:Standard error of the mean; TLR5:Toll-like receptor 5; TLRs:Toll-like receptors; TNF-α:Tumor necrosis factor-α; WT:Wild-type

Declarations

Availability of data and materials

All materials are commercially available, and the datasets used and/or analyzed during the current study are available from the corresponding author on reasonable request.

Ethics approval and consent to participate

All animal experiments were approved by the Institutional Animal Care and Use Committee of the Beijing Institute of Lifeomics (NO. IACUC-DWZX-2020-568).

Consent for publication

Not applicable.

Competing interests

The authors declare that they have no competing interests.

Funding

This work was supported by grants from the National Natural Science Foundation of China (81800561), the State Key Laboratory of Proteomics (SKLP-K201404).

Authors' contributions

WZ conducted the experiments. LW, XHS, XL, YX, JZ, TW, YTL collected and analyzed the data. HC, YQZ, MY, CHG, CYL gave technical or material support. GMR contributed to the study design. WZ, RHY, and XMY drafted the manuscript. XMY and RHY supervised the project. LW and MY obtained funding. All authors read and approved the final manuscript.

Acknowledgements

We thank Prof. Huimin Yan for kindly providing *Tlr5*$^{-/-}$ mice.

References

1. Michalopoulos GK, Defrances MC. Liver Regeneration. Adv Biochem Eng Biotechnol. 2005;93(5309):101–34.
2. Fausto N. Liver regeneration. J Hepatol. 2000;32:19–31.
3. Fausto N, Laird AD, Webber EM. Liver regeneration. 2. Role of growth factors and cytokines in hepatic regeneration. Faseb Journal Official Publication of the Federation of American Societies for Experimental Biology. 1995;9(15):1527–36.
4. Blindenbacher A, Wang X, Langer I, Savino R, Terracciano L, Heim MH. Interleukin 6 is important for survival after partial hepatectomy in mice. Hepatology. 2003;38:674–82.
5. Gallucci, Simeonova RM, Toriumi PP, Luster W. M. I. TNF-alpha regulates transforming growth factor-alpha expression in regenerating murine liver and isolated hepatocytes. J Immunol. 2000;164(2):872–8.
6. Taub R. Liver regeneration: from myth to mechanism. Nat Rev Mol Cell Biol. 2004;5(10):836–47.
7. Seki E, Park EJ, Fujimoto J. Toll-like receptor signaling in liver regeneration, fibrosis and carcinogenesis. Hepatol Res. 2011;41(7):597–610.
8. Wu J, Meng Z, Jiang M, Zhang E, Trippler M, Broering R, et al. Toll-like receptor-induced innate immune responses in non-parenchymal liver cells are cell type-specific. Immunology. 2009;129(3):363–74.

9. Jiang DH, Liang JR, Fan J, Yu S, Chen SP, Luo Y, et al. Regulation of lung injury and repair by Toll-like receptors and hyaluronan. Nat Med. 2005;11(11):1173–9.
10. Galluzzi L, Vacchelli E, Eggermont A, Fridman WH, Kroemer G. Trial Watch: Experimental Toll-like receptor agonists for cancer therapy. Oncoimmunology. 2012;1(5):699–716.
11. Lin Q, Li M, Fang D, Fang J, Su SB. The essential roles of Toll-like receptor signaling pathways in sterile inflammatory diseases. Int Immunopharmacol. 2011;11(10):1422–32.
12. Kawai T, Akira S. TLR signaling; proceedings of the Semin Immunol, F, 2007 [C].
13. O'neill LA. How Toll-like receptors signal: what we know and what we don't know. Curr Opin Immunol. 2006;18(1):3–9.
14. Seki E, Tsutsui H, Iimuro Y, Naka T, Son G, Akira S, et al. Contribution of Toll-like receptor/myeloid differentiation factor 88 signaling to murine liver regeneration. Hepatology. 2005;41(3):443–50.
15. Campbell JS, Riehle KJ, Brooling JT, Bauer RL, Mitchell C, Fausto N. Proinflammatory Cytokine Production in Liver Regeneration Is Myd88-Dependent, but Independent of Cd14, Tlr2, and Tlr4. J Immunol. 2006;176(4):2522–8.
16. Zorde-Khvalevsky E, Abramovitch R, Barash H, Spivak-Pohis I, Rivkin L, Rachmilewitz J, et al. Toll-like receptor 3 signaling attenuates liver regeneration. 2009;50(1):198–206.
17. Burdelya LG, Krivokrysenko VI, Tallant TC, Strom E, Gleiberman AS, Gupta D, et al. An Agonist of Toll-Like Receptor 5 Has Radioprotective Activity in Mouse and Primate Models. Science. 2008;320(5873):226–30.
18. Hao B, Feifei S, Ganggang Y, Lei W, Quanyi Z, Quanhai Z, et al. CBLB502, a toll-like receptor 5 agonist, offers protection against Radiation-Induced male reproductive system damage in mice. Biol Reprod. 2018;100.
19. Didierlaurent A, Ferrero I, Otten LA, Dubois B, Reinhardt M, Carlsen H, et al. Flagellin Promotes Myeloid Differentiation Factor 88-Dependent Development of Th2-Type Response. J Immunol. 2004;172(11):6922–30.
20. Hao J, Zhang C, Liang T, Song J, Hou G. rFliC prolongs allograft survival in association with the activation of recipient Tregs in a TLR5-dependent manner. Cell Mol Immunol. 2014;11(002):206–14.
21. Hossain MS, Ramachandiran S, Gewirtz AT, Waller EK. Recombinant TLR5 Agonist CBLB502 Promotes NK Cell-Mediated Anti-CMV Immunity in Mice. PLoS One. 2014;9(5):e96165.
22. Burdelya LG, Brackett CM, Kojouharov B, Gitlin II, Leonova KI, Gleiberman AS, et al. Central role of liver in anticancer and radioprotective activities of Toll-like receptor 5 agonist. Proc Natl Acad Sci U S A. 2013;110(20):E1857-E66.
23. Wang L, Zhang W, Ge C-H, Yin R-H, Xiao Y. Toll-like receptor 5 signaling restrains T-cell/natural killer T-cell activation and protects against concanavalin A-induced hepatic injury. Hepatology. 2017;65:2059–73.
24. Leigh ND, Bian G, Ding X, Liu H, Aygun-Sunar S, Burdelya LG, et al. A Flagellin-Derived Toll-Like Receptor 5 Agonist Stimulates Cytotoxic Lymphocyte-Mediated Tumor Immunity. PLoS One.

2014;9(1):e85587.

25. Kawai T, Akira S. The role of pattern-recognition receptors in innate immunity: update on Toll-like receptors. Nat Immunol. 2010;11(5):373–84.
26. Fausto N, Campbell JS, Riehle KJ. Liver regeneration. Hepatology. 2006;43:45–53.
27. Higgins GM, Anderson RM. Experimental pathology of the liver. I. Restoration of the liver of the white rat following partial surgical removal. Arch Pathol. 1931;12:186–202.
28. Liu X, Han M, Zhao C, Chang C, Zhu Y, Ge C, et al. KeggExp: a web server for visual integration of KEGG pathways and expression profile data. Bioinformatics. 2018;35(8):1430–2.
29. Rib L, Villeneuve D, Minocha S, Praz V, Hernandez N, Guex N, et al. Cycles of gene expression and genome response during mammalian tissue regeneration. Epigenetics chromatin. 2018;11(1):52.
30. Zhang X-J, Wang B, Olsavszky V, Schledzewski K, Hartmann D. Hepatic angiocrine HGF signaling plays a vital role in the early stage of liver regeneration after PHx in mice. HPB (Oxford). 2018;20(2):483.
31. Tomiya T, Fujiwara K. Trends in Gastroenterology and Hepatology: Significance of the Relation Between Hepatocyte Growth Factor and Transforming Growth Factor-α in Hepatocyte Proliferation [M]. Springer Japan, 2001.
32. Glende EA, Morgan WS. Alteration in liver lipid and lipid fatty acid composition after partial hepatectomy in the rat. Exp Mol Pathol. 1968;8(2):190–200.
33. Delahunty TJ, Rubinstein D. Accumulation and release of triglycerides by rat liver following partial hepatectomy. J Lipid Res. 1970;11(6):536–43.
34. Girard A, Roheim PS, Eder HA. Lipoproten synthesis and fatty acid mobilization in rats after partial hepatectomy. Biochim Biophys Acta. 1971;248(1):105–13.
35. Shu M, Huang DD, Hung ZA, Hu XR, Zhang S. Inhibition of MAPK and NF-κB signaling pathways alleviate carbon tetrachloride (CCl4)-induced liver fibrosis in Toll-like receptor 5 (TLR5) deficiency mice. Biochem Biophys Res Commun. 2016;471(1):233–9.
36. Etienne-Mesmin L, Vijay-Kumar M, Gewirtz AT, Chassaing B. Hepatocyte Toll-Like Receptor 5 Promotes Bacterial Clearance and Protects Mice Against High-Fat Diet-Induced Liver Disease. Cell Mol Gastroenterol Hepatol. 2016;2(5):584–604.
37. Matsumura T, Degawa T, Takii T, Hayashi H, Okamoto T, Inoue J, et al. TRAF6-NF-kappaB pathway is essential for interleukin-1-induced TLR2 expression and its functional response to TLR2 ligand in murine hepatocytes. Immunology. 2003;109(1):127–36.
38. Yang L, Magness ST, Bataller R, Rippe RA, Brenner DA. NF-kappa B activation in Kupffer cells after partial hepatectomy. American Journal of Physiology Gastrointestinal Liver Physiology. 2005;289(3):G530-G8.
39. Kiyoshi N, Hiroyuki, Nakashima, Masami I, et al. Mouse CD11b + Kupffer Cells Recruited from Bone Marrow Accelerate Liver Regeneration after Partial Hepatectomy. PLoS One. 2015;10:e0136774.

40. Yin S, Wang H, Park O, Wei W, Shen J, Gao B. Enhanced liver regeneration in IL-10-deficient mice after partial hepatectomy via stimulating inflammatory response and activating hepatocyte STAT3. Am J Pathol. 2011;178(4):1614–21.
41. Fausto N. Growth factors in liver development, regeneration and carcinogenesis. Prog Growth Factor Res. 1991;3(3):219–34.
42. Michalopoulos G. HGF and liver regeneration. Gastroenterol Jpn. 1993;28(Suppl 4(4):36–9.
43. Oishi K, Hayamizu K, Aihaiti X, Itamoto T, Arihiro K, Asahara T. G-CSF-induced evacuation of sinusoidal NK cells and the facilitation of liver regeneration in a partial hepatectomy. Cytokine. 2006;34(1–2):66–75.
44. Grandini E. Evaluation of the efficacy of intrahepatic autologous stem cells (SC) CD133 + infusion in patients with cirrhosis and advanced hepatic insufficiency. 2014.
45. Shteyer E, Liao Y, Muglia LJ, Hruz PW, Rudnick DA. Disruption of hepatic adipogenesis is associated with impaired liver regeneration in mice. Hepatology. 2004;40(6):1322–32.

Figures

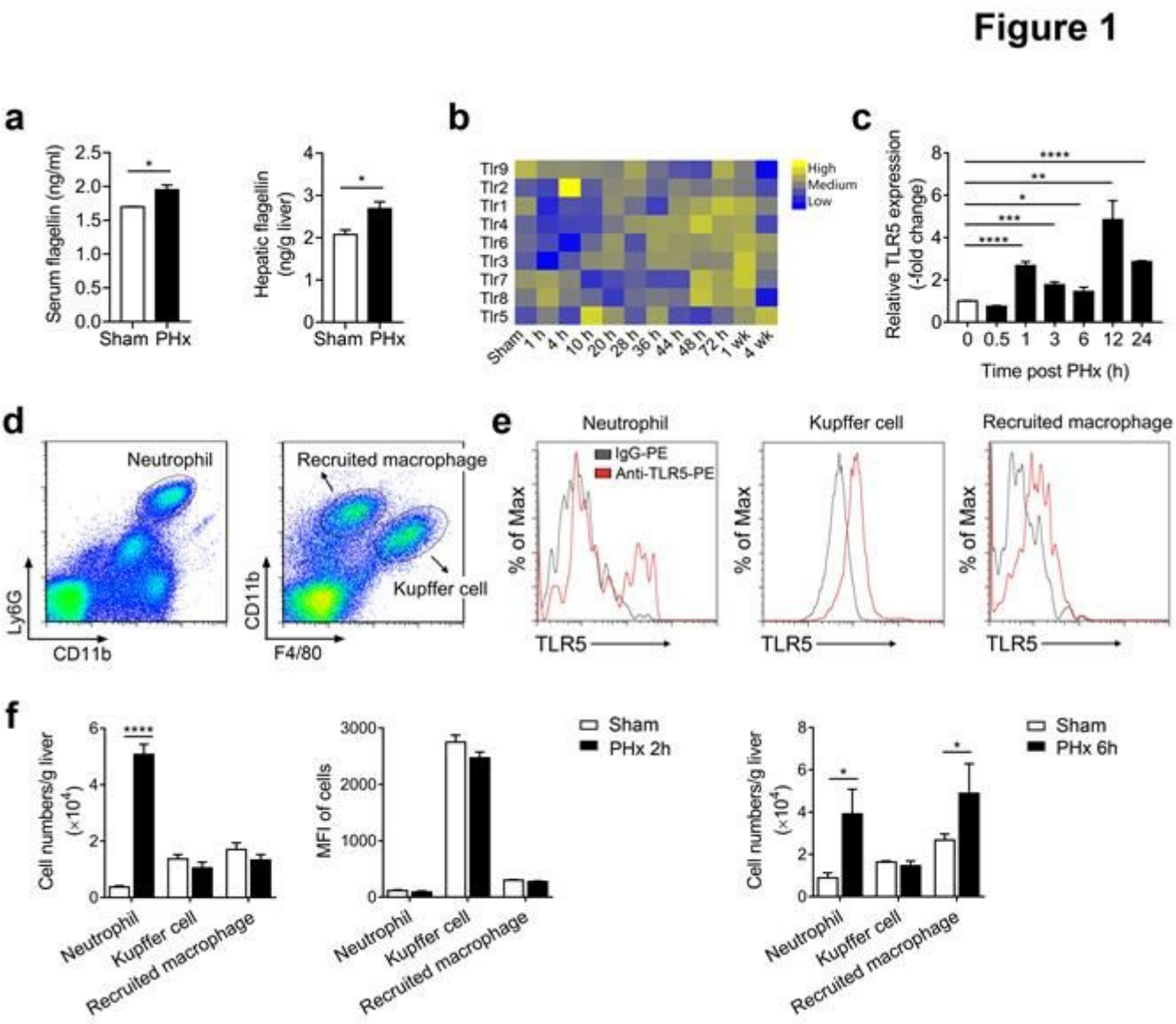

Figure 1

TLR5 is up-regulated in the liver after PHx. a. Flagellin concentrations in serum and liver of WT mice 6 hours following sham surgery or PHx. b. TLRs expression levels in regenerating WT mice liver upon PHx from published transcriptome dataset (GSE95135). c. Relative mRNA levels of hepatic TLR5 at the indicated times following PHx (n = 3 replicates). Flow cytometry gating strategy (d) and TLR5 expression levels (e) of liver neutrophils, KCs and recruited macrophages in WT mice. f. Cell counts and mean fluorescence intensity of liver neutrophils, KCs, and recruited macrophages at the indicated times upon PHx. Data are presented as mean ± SEM; n = 3-6 per group. *P < 0.05, **P <0.01, ***P <0.001, ****P <0.0001; two-tailed unpaired t-test.

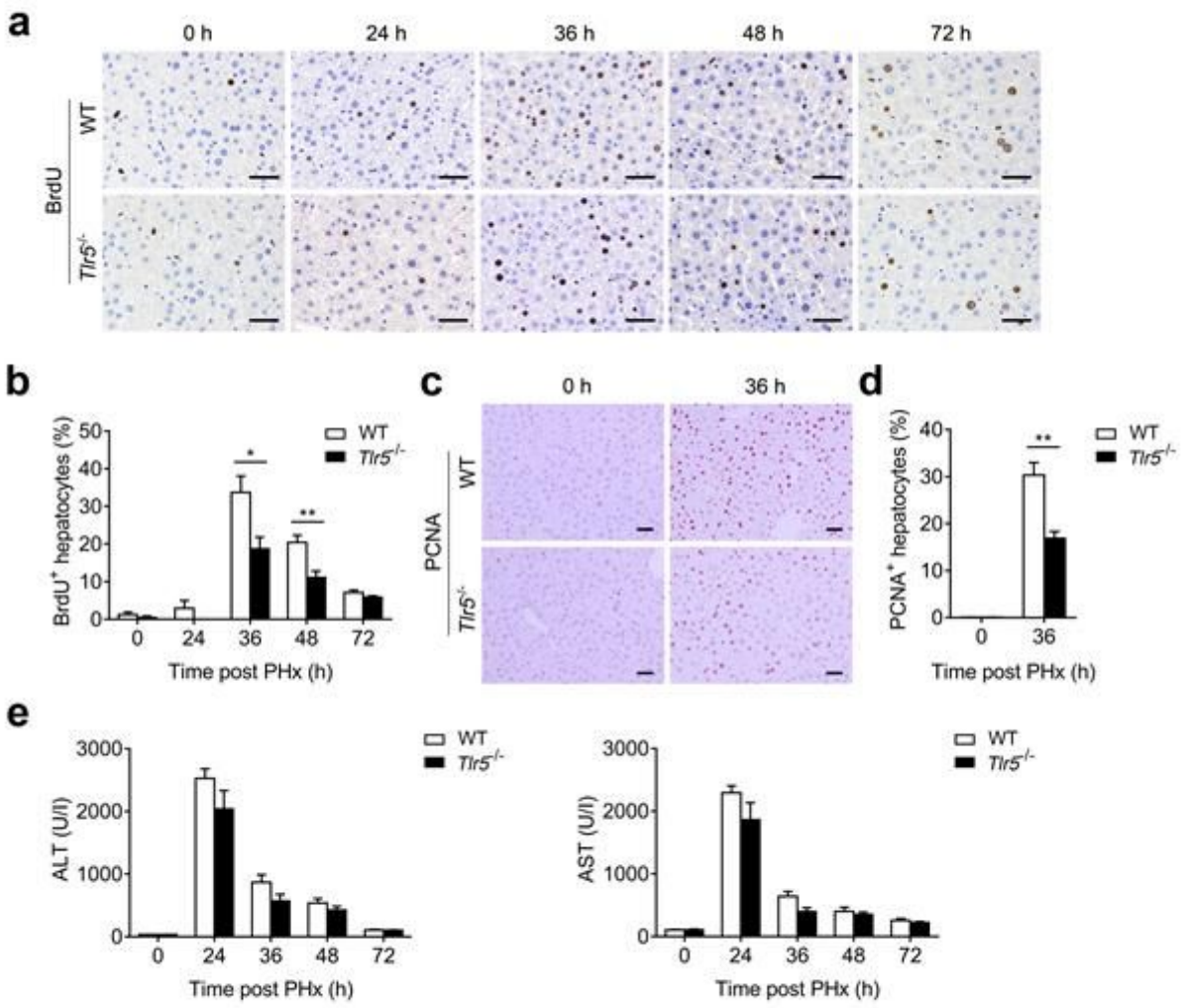

Figure 2

TLR5 deficiency attenuates hepatocyte proliferation following PHx. PHx was performed on WT and Tlr5−/− mice. Proliferation was measured by BrdU and PCNA immunohistochemistry staining. Representative IHC staining images were shown (a and c), and the percentage of BrdU-positive cells (b) and PCNA-positive cells (d) were counted. e. Serum ALT and AST level of WT and Tlr5−/− mice subjected to PHx. Scale bar, 50 μm. Data are presented as mean ± SEM; n = 5-6 per group. *P < 0.05, **P <0.01; two-tailed unpaired t-test.

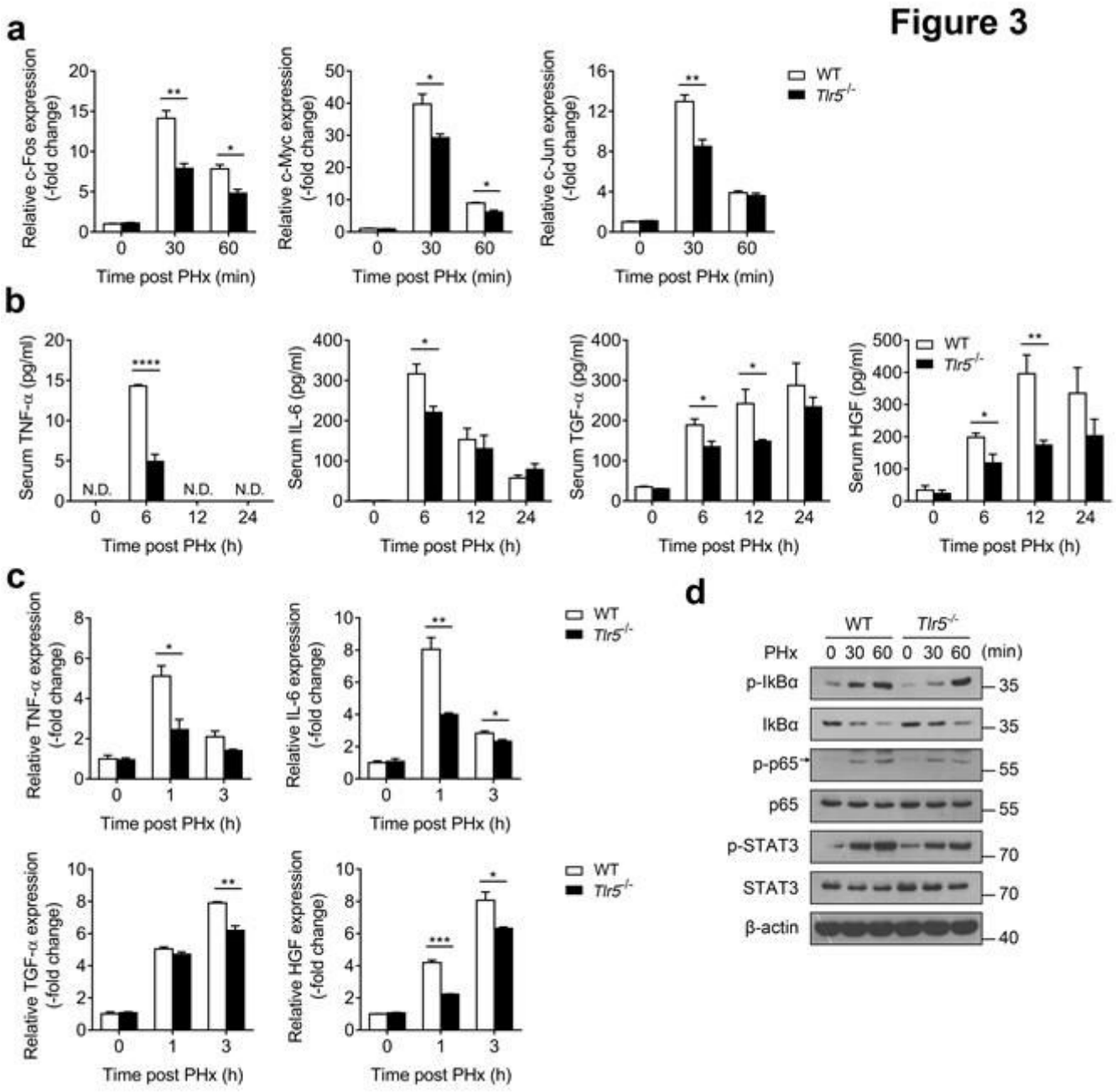

Figure 3

TLR5 deficiency suppresses hepatocyte priming in PHx-induced liver regeneration. a. Relative mRNA levels of hepatic c-fos, c-myc, and c-jun in WT and Tlr5−/− mice at the indicated times after PHx. b. Serum levels of TNF-α, IL-6, TGF-α, HGF were measured in regenerating WT and Tlr5−/− mice liver. c. Quantification of hepatic TNF-α, IL-6, TGF-α, and HGF mRNA expression in WT and Tlr5−/− mice at the indicated times after PHx. d. Western blot analysis of the indicated target proteins in WT and Tlr5−/− mice liver after PHx with β-actin as loading control (n = 3 replicates). Data are presented as mean ± SEM; n = 4-6 per group. *P < 0.05, **P <0.01, ***P <0.001, ****P <0.0001; two-tailed unpaired t-test. N.D., not detected.

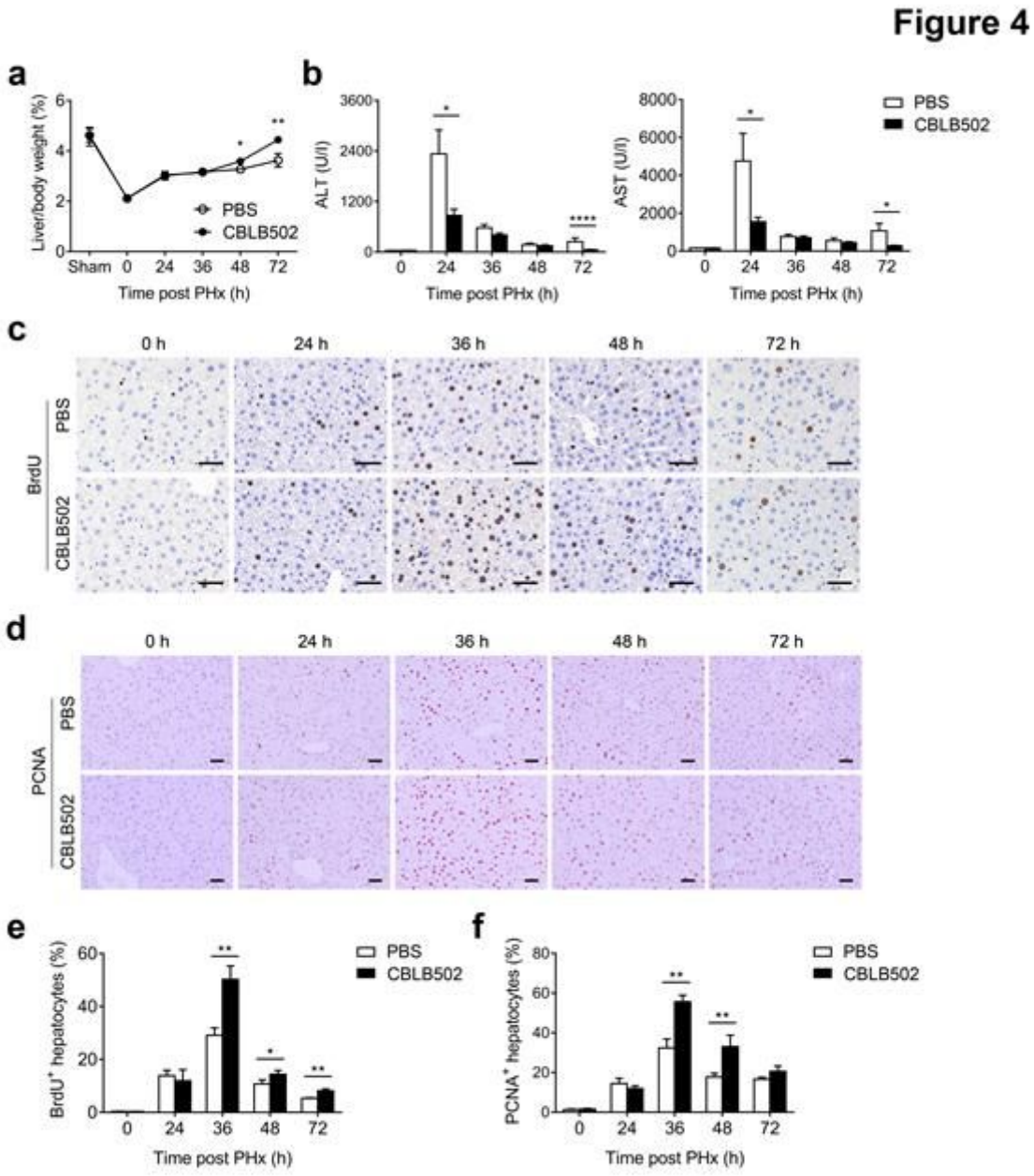

Figure 4

The TLR5 agonist CBLB502 enhances hepatocyte proliferation in mice following PHx. Liver to body weight ratio (a), serum ALT and AST level (b) of PBS and CBLB502 treated mice after PHx. Hepatocyte proliferation was measured by BrdU (c) and PCNA (d) immunohistochemistry staining. The percentage of BrdU-positive cells (e) and PCNA-positive cells (f) were counted at the indicated times after PHx. Scale bar, 50 μm. Data are presented as mean ± SEM; n = 6-12 per group. *P < 0.05, **P <0.01, ****P <0.0001; two-tailed unpaired t-test.

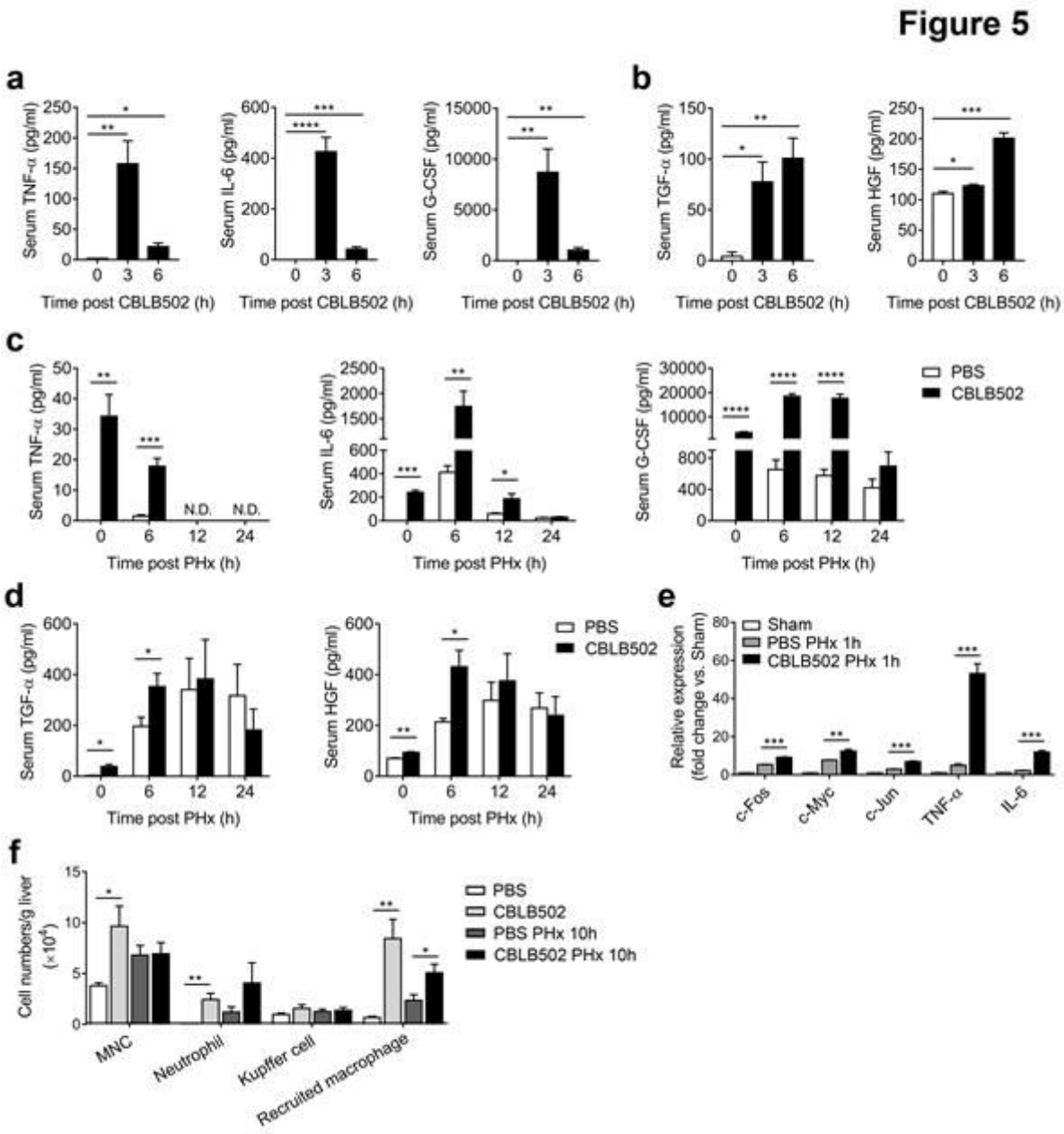

Figure 5

Enhanced inflammatory response in CBLB502-pretreated mice after PHx. Serum levels of TNF-α, IL-6, G-CSF (a), TGF-α, HGF (b) in CBLB502 treated mice at the indicated times. Serum levels of TNF-α, IL-6, G-CSF (c), TGF-α, and HGF (d) were measured in regenerating PBS and CBLB502 treated mice liver after PHx. e. Relative mRNA levels of hepatic c-Fos, c-Myc, c-Jun, TNF-α, and IL-6 in PBS and CBLB502 treated mice upon PHx. f. Cell counts of liver MNCs, neutrophils, KCs, and recruited macrophages in PBS and CBLB502 treated mice following sham surgery or PHx. Data are presented as mean ± SEM; n = 3-7 per group. *P < 0.05, **P <0.01, ***P <0.001, ****P <0.0001; two-tailed unpaired t-test. N.D., not detected.

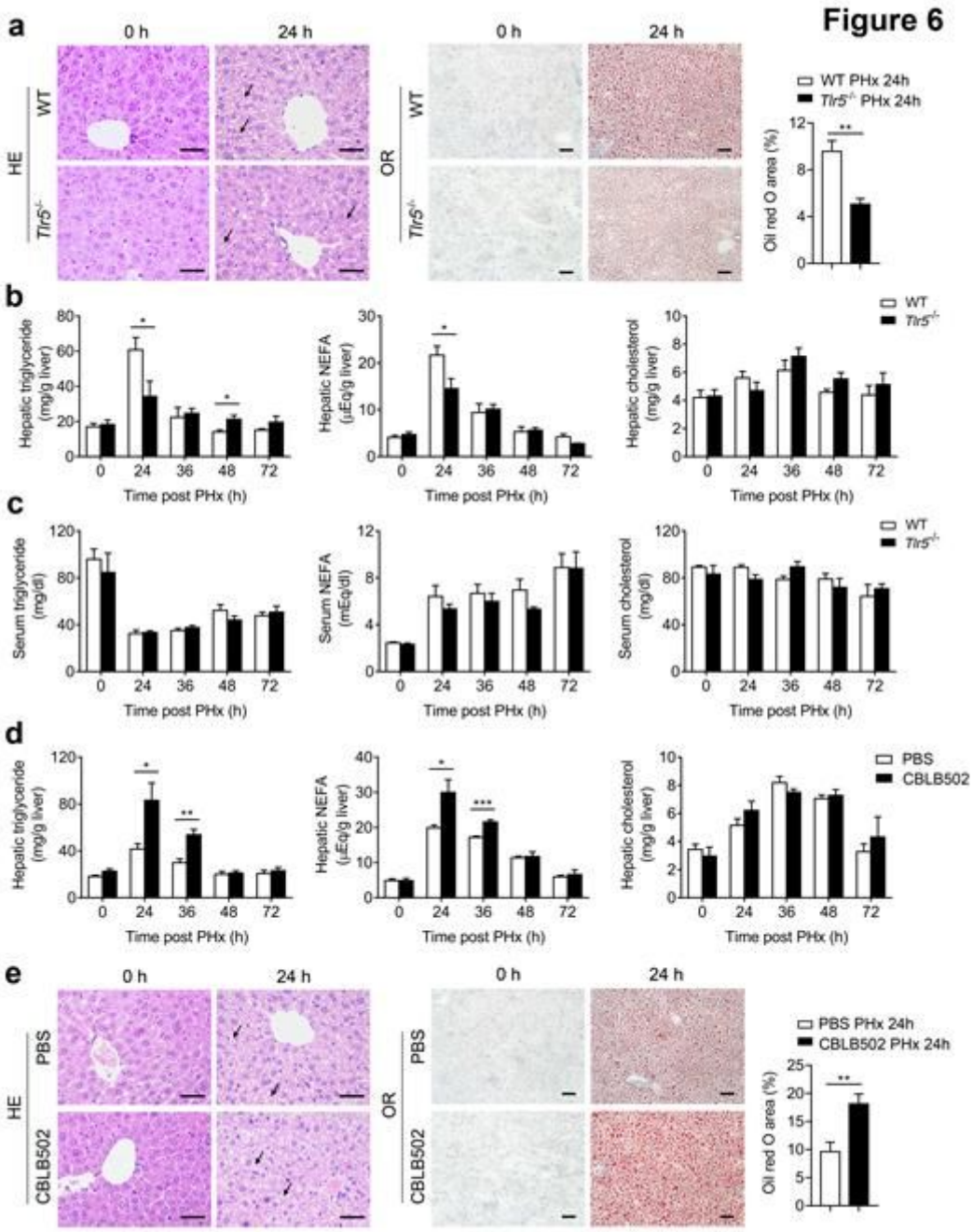

Figure 6

TLR5 signaling contributes to hepatic lipid accumulation induced by PHx. a. H&E staining, Oil Red O staining, and quantification of Oil Red O positive areas of WT and Tlr5−/− mice livers upon PHx. Triglyceride, NEFA, and cholesterol levels in liver extracts (b) and serum (c) were measured in WT and Tlr5−/− mice at the indicated times after PHx. d. Analysis of hepatic triglyceride, NEFA, and cholesterol level in PBS and CBLB502 treated mice upon PHx. e. H&E staining, Oil Red O staining, and quantification of Oil Red O positive areas of PBS and CBLB502 treated mice livers following PHx. Black arrows indicate hepatic lipid. Scale bar, 50 μm. Data are presented as mean ± SEM; n = 5-7 per group. *P < 0.05, **P <0.01, ***P <0.001; two-tailed unpaired t-test.

Supplementary Files

This is a list of supplementary files associated with this preprint. Click to download.

- SupplementaryInformation.docx